Journal of Physical Science Vol. 36(2), 61–80, 2025



Reinforcement of PMMA Denture Base Properties with Hybrid Nanofillers

Issam Mohahed Aldwimi, ^{1,2,3} Hazizan Md Akil, ^{1,2*} Zuratul Ain Abdul Hamid^{1,2} and Ahmed Omran Alhareb^{1,3}

¹School of Materials and Mineral Resources Engineering, Universiti Sains Malaysia, Engineering Campus, 14300 Nibong Tebal, Pulau Pinang, Malaysia ²Cluster of Polymer Composites, Universiti Sains Malaysia, 14300 Nibong Tebal, ⁹Pulau Pinang, Malaysia

The Faculty of Medical Technology of Msellata, Almergib University, Libya

*Corresponding author: hazizan@usm.my

Published online: 29 August 2025

To cite this article: Aldwimi, I. M. et al. (2025). Reinforcement of PMMA denture base properties with hybrid nanofillers. *J. Phys. Sci.*, 36(2), 61–80. https://doi.org/10.21315/jps2025.36.2.4

To link this article: https://doi.org/10.21315/jps2025.36.2.4

ABSTRACT: The study aimed to enhance the mechanical properties of polymethyl methacrylate (PMMA) by developing nanocomposites incorporating halloysite nanotubes (HNTs) and multi-walled carbon nanotubes (MWCNTs). These hybrid nanofillers, fixed at 5 wt.%, were assessed for their impact on PMMA's impact strength (IS) and fracture toughness (KIC). After surface treatment with a silane coupling agent, their properties were analysed using field emission scanning electron microscopy (FESEM). The results showed significant improvements (p < 0.05) in IS and KIC with increasing MWCNT concentration. Notably, a ratio of 4.25 wt.% HNTs to 0.75 wt.% MWCNTs yielded the greatest enhancement, with IS and KIC values of 10.26 kJm $^{-2}$ and 2.59 MPa·m $^{1/2}$, respectively, compared to pure PMMA. These findings suggest that hybrid nanofillers can potentially improve PMMA denture bases, enhancing the durability of dental composites.

Keywords: PMMA, HNTs, MWCNTs, impact strength, fracture toughness

1. INTRODUCTION

In recent decades, significant progress in dental biomaterials research has led to substantial improvements in the properties and performance of dental materials and restorative techniques. A key focus has been the development of innovative materials with enhanced biological and mechanical characteristics. This includes the utilisation of nanotechnology and the advancement of novel materials such as zirconia and other ceramics, which offer superiour strength, durability and biocompatibility compared to traditional materials. Materials lacking biocompatibility can trigger inflammation, tissue damage and other adverse effects, potentially leading to implant failure or

complications. Another major challenge in dental prosthetics and restorations is achieving a natural appearance, as patients expect seamless integration of restorations with their natural teeth and gums.²

Polymethyl methacrylate (PMMA) enjoys widespread use within the dental field because of its ease of processing, lightweight nature, affordability, ability to adhere to teeth, aesthetic qualities and stability within the oral environment.³ Furthermore, PMMA demonstrates biocompatibility, ensuring its safe application in the oral cavity.^{4,5} In dentistry, PMMA-based materials play a pivotal role in removable dentures, a common solution for missing teeth. Furthermore, PMMA's versatility extends beyond the realm of dentistry and medicine. Its transparency and impressive impact resistance render it a popular choice for transparent alternatives to glass, such as in aquariums and display cases.^{4,6,7}

However, PMMA resin exhibits certain drawbacks concerning its mechanical characteristics, making it less suitable for specific dental applications.⁸ To illustrate, its limited flexural strength can result in material fractures or fissures over time, while its diminished impact resistance makes it more vulnerable to damage from accidental drops or impacts.^{9,10} Furthermore, although maxillary dentures offer functional and cosmetic solutions for individuals with missing teeth, they can be at risk of fracture or breakage in specific situations, such as midline fracture.^{11–13} To mitigate the risk of fractures, dentures must excel in terms of properties, necessitating the ability to withstand forces associated with normal oral function without experiencing breakage or cracking.¹⁴ The field of dental materials has seen technological advancements, resulting in new dentures featuring enhanced properties, including high-impact and reinforced composites. These materials provide improved durability and resistance to fractures compared to traditional materials.^{15–17}

Recently, nanotechnology has opened up fresh opportunities for enhancing materials, including polymeric nanocomposites. ¹⁸ These composites are crafted by integrating nanoscale fillers into a polymer, which can result in improved properties and other advantages. One notable benefit of polymeric nanocomposites is that the minuscule size of the filler particles yields a larger surface area, potentially enhancing the material's strength and hardness. ¹⁹ These materials have displayed promising outcomes in specific instances, such as increased wear resistance and bonding strength. ²⁰ Nanoscale reinforcing has demonstrated the ability to introduce novel physical, mechanical and biomedical attributes and enhance biocompatibility when incorporated into PMMA nanocomposites. ^{4,21} This study focused on improving the PMMA base mechanical properties, such as impact strength (IS) and fracture toughness (K_{IC}) through the use of a mixture of treated halloysite nanotubes (HNTs) and MWCNTs nanofillers.

2. MATERIALS AND METHODS

2.1 Materials

In the current investigation, the materials employed included PMMA (Aldrich U.S.A) combined with 0.5% benzoyl peroxide (BPO) (Merck, Germany). The liquid components comprised a mixture of 90% methyl methacrylate (MMA) (Flucka, UK) stabilised with 0.005% hydroquinone and 10% ethylene glycol dimethacrylate (EGDMA) (Aldrich U.S.A.). The hybrid nanofillers were used to reinforce PMMA composites, including HNTs (Aldrich U.S.A.) and MWCNTs (Aldrich U.S.A.). To improve the interaction between PMMA and nanofillers, the Silane (3-trimethoxysilyl propylmethacrylate [γ -MPS]), was employed in their treatment (Sigma-Aldrich, Germany).

2.2 Salinisation Process of Nanofillers Surface

The salinisation process began by dispersing 10 g of nanofiller powder (HNTs or MWCNTs) in 200 mL of toluene. Silane coupling agent was added to powder at a concentration of 10 wt.% at room temperature. The mixture was continuously stirred at 150 rotations per minute for 15 h. The solution was then filtered to separate and collect the modified powder from the liquid. The collected modified nanofiller powder was cleansed using a Soxhlet apparatus with 300 mL of fresh toluene over 24 h. Finally, the modified powder was dried in a vacuum oven at 110°C for 3 h to remove any remaining solvent.

2.3 Preparation of the PMMA Denture Base Composite

The composite was prepared using powder components containing PMMA and 0.5 wt.% BPO, along with a liquid mixture of 90% MMA and 10% EGMMAS. A small amount of hydroquinone (0.025%) was added to the liquid to control polymerisation. Nanofillers (HNTs/MWCNTs) were added at different concentrations (see Table 1) and dispersed in MMA monomer using ultrasonication before blending with the composite. Ultrasonication is extensively employed to achieve homogeneous dispersion of nanoparticles in liquid media. The underlying mechanism involves the use of high-frequency sound waves, typically ranging from 20 kHz to several hundred kHz, which agitate the particles within the liquid. This agitation induces cavitation, the rapid formation and collapse of microscopic bubbles. Upon collapse, these bubbles release localised energy in the form of heat and pressure, which serves to disintegrate agglomerated nanoparticles, ensuring even dispersion. In practice, the nanoparticle mixture is first introduced into a MMA

solution, followed by ultrasonic treatment for 5 min. During this process, a high-frequency ultrasonic probe or bath directs sound waves into the liquid, generating cavitation that effectively breaks apart and uniformly disperses the nanoparticles throughout the MMA medium. Ultrasonication minimises the risk of nanoparticle agglomeration, sedimentation and phase separation, all of which could compromise the uniformity of the material. Consequently, the process enhances the homogeneity and overall quality of the final product. After the 5 min treatment, the nanoparticle-dispersed MMA solution is ready for subsequent processing or mixing steps.

The mixture reached the dough stage for 15 min and was then packed into moulds. The moulds were pressed at 14MPa pressure for 35 min. Polymerisation occurred by immersing the moulds in a 79°C water bath for 90 min, forming rigid samples. After cooling at room temperature, finishing and polishing were done using an X35 handpiece or 240 emery paper.

TC 11	4	c ·		1	1.
Lable	1:	Specimen	grouping	and	coding.
		- I	0 1 0		0

Group/Subgroup	Powder (wt.%)				Liquid	
Code	PMMA	BPO	HNTS	MWCTs	MMA (%)	EGDMA (%)
G1	99.50	0.50	_	_	90	10
G2	94.50	0.50	4.75	0.25	90	10
G3	94.50	0.50	4.50	0.50	90	10
G4	94.50	0.50	4.25	0.75	90	10
G5	94.50	0.50	4.00	1.00	90	10
G6	94.50	0.50	3.50	1.50	90	10
G7	94.50	0.50	2.50	2.50	90	10

Note: G1 = PMMA matrix; G2 = PMMA matrix with 4.75 wt.% HNTs + 0.25 wt.% MWCNTs; G3 = PMMA matrix with 4.50 wt.% HNTs + 0.50 wt.% MWCNTs; G4 = PMMA matrix with 4.25 wt.% HNTs + 0.75 wt.% MWCNTs; G5 = PMMA matrix with 4.00 wt.% HNTs + 1.00 wt.% MWCNTs; G6 = PMMA matrix with 3.50 wt.% HNTs + 1.50 wt.% MWCNTs; G7 = PMMA matrix with 2.50 wt.% HNTs + 2.50 wt.% MWCNTs.

2.4 Specimen Preparation

2.4.1 Impact strength

ISO 179-1:2023 is an international standard that delineates a procedure for assessing the IS of plastic materials through the Charpy V-notch test. In this examination, the sample has dimensions of 80 mm in length, 10 mm in width, 9.75 mm in width beneath the V-notch, which has a radius of 0.25 mm and an angle of 45°, and a

thickness of 4 mm. The test is carried out using a notched bar for IS measurement with a span support of 62 mm. The mean impact strength of samples is determined using Equation 1;

$$IS = \frac{E}{b_n d} \times 10^3 \tag{1}$$

where,

E = energy value absorbed by the sample during the impact test in joules

 b_n = sample width

d = sample thickness

2.4.2 Fracture toughness

The assessment of the material fracture toughness (K_{IC}) was carried out through the execution of the single edge span notch bending test as prescribed in ISO 13586:2018 standard. The specimen dimensions; a length of 80 mm, notch length of 4 mm, span length of 64 mm, thickness of 4 mm and width of 20 mm. To create the notch in the sample, a razor blade was employed, resulting in the notch that included a loading nose, a supporting span of 50 mm, and two supports with diameters of 20 mm and 10 mm. The testing was carried out with a crosshead speed set at 1.00 mmmin⁻¹ and applying a load of 10KN to samples. The K_{IC} values were determined by Equation 2, and the geometric factor (y) was calculated utilising Equation 3.

$$K_{IC} = \frac{P\frac{S}{2}a^{\frac{1}{2}}}{t\frac{W^2}{3}}y\tag{2}$$

$$y = 1.93 - 3.07 \left(\frac{a}{w}\right) + 14.53 \left(\frac{a}{w}\right)^2 - 25.11 \left(\frac{a}{w}\right)^3 + 25.8 \left(\frac{a}{w}\right)^4$$
 (3)

where,

P = represents the load at the peak

S = span length

a =notch length

t = sample thickness

w = sample width

2.4.3 Artificial saliva absorption

An artificial saliva absorption (ASA) test was employed to evaluate the performance of dental materials. These assessments adhere to ISO 1567-2005 standards, which outline the necessary procedures and criteria. PMMA samples are fabricated in stainless steel moulds with a depth of 3 mm and a diameter of 50 mm. The samples undergo a conditioning process; they are placed in desiccators with silica gel at 37°C for 23 h, followed by 23°C for 60 min, and this cycle is repeated until a constant mass (m_1) is reached. The weight loss during this process must remain below 0.2 mg. To determine the volume of PMMA samples for each formulation, the average sample area and thickness are employed to calculate their dimensions and subsequently, their volume. Subsequently, the PMMA samples are submerged in artificial saliva at 37°C, maintaining a 3 mm separation between each sample for durations of 1 day, 3 days, 7 days, 14 days, 21 days and 28 days. After removing them from the liquid, the samples are dried, waved in the air for 15 s, and then weighed using an analytical balance 60 s after being taken out of the solution. The weight of the samples is recorded as (m_2) . The samples are then reconditioned to a constant mass through repeated cycles of immersion and drying. They are placed in desiccators with fresh silica gel at 37°C for 23 h, and this process is repeated until the mass loss is less than 0.0001 g during any 23 h. The resulting constant mass is noted as (m_3) . The AS absorption (measured in µgmm⁻³) and the percentage of weight loss are subsequently computed in compliance with ISO 1567-2005, utilising Equations 4 and 5.

$$AS \ absorption = \frac{m_2 - m_3}{V} \tag{4}$$

Loss of weight =
$$\frac{m_3 - m_1}{V} \times 100$$
 (5)

where,

AS = artificial saliva

 m_1 = the conditioned mass (µg) before immersion in AS

 m_2 = the conditioned mass of the samples (µg) after immersion in AS

 m_3 = the reconditioned mass (µg) after drying

V = the volume of the samples (mm³)

2.4.4 Morphology and chemical microanalysis of filler particles

The scanning electron microscope (SEM) was used for the examination of fractured specimen surfaces. To prepare samples for field emission scanning electron microscopy (FESEM), a Bio-Red E5000 Sputter Coater from the USA was employed to apply a thin metallic layer. This step was taken to improve the clarity of images and prevent electrostatic charging issues. Different aspects of particle surfaces could be investigated by adjusting electron beam voltage within the typical range of 5 kV–50 kV during the acquisition of micrographs. Lower voltages were used for examining surface features, whereas higher voltages were applied to facilitate the study of subsurface characteristics.

3. STATISTICAL ANALYSIS

In this study, One-way analysis of variance (ANOVA) along with Tukey's post hoc analysis was used. ANOVA was applied to analyse the data of IS and K_{IC} to identify any noteworthy distinctions among the different groups (P < 0.05).

4. RESULTS AND DISCUSSION

4.1 Confirmation of the Effect of Silane Coupling Agent Treatment of the Fillers

Figures 1 and 2 depict the outcomes of FESEM micrographs and energy-dispersive X-ray spectroscopy (EDX) analysis for HNTs and MWCNTs nano-powder, both pre-silane and post-silane treatment. These visuals illustrate alterations in the surface structure and chemical composition of the ceramic fillers after undergoing the silane treatment procedure. The FESEM micrographs reveal shifts in surface morphology, while the EDX analysis highlights changes in the sample's chemical makeup. The EDX analysis indicates the utilisation of a silane coupling agent to treat the nanofillers in the HNTs/MWCNTs/PMMA composite, a common practice in composite production. Silane coupling agents serve to enhance the interaction between the filler and matrix materials, ultimately resulting in improved mechanical properties. The detection of silicon (Si) elements at the filler-matrix interface provides concrete evidence of the silane coupling agent's presence. Additionally, assessing the weight and atom percentages of the filler elements and Si can offer further insights into the effectiveness of this treatment.²² Simultaneously, silane coupling agents find application in enhancing the properties of polymer composites by fostering chemical bonds between filler particles and the matrix. These chemical bonds enhance the interaction and adhesion between filler particles and the polymer, leading to enhancements in the composite material's properties. 23,24

FESEM offers a means to obtain highly detailed images of a material's surface, allowing us to examine the structural characteristics of particles within the composite. Specifically, when assessing the 5 wt.% MWCNTs and HNTs in MWCNTs/PMMA and HNTs/PMMA composites, FESEM enables the observation of their shapes, dimensions and distribution in the composite. In the case of the 5 wt.% MWCNTs and HNTs within the MWCNTs/HNTs/PMMA composite, EDX serves as a tool for confirming the presence of carbon and other elements within the MWCNTs and HNTs. Additionally, EDX can be utilised to quantify the relative concentrations of these elements in the composite, thereby providing valuable insights into the efficacy of the treatment process. The identification of the Si group in both the MWCNTs/PMMA and HNTs/PMMA composites indicates the successful treatment of ceramic fillers with a silane coupling agent, thus confirming the treatment process's effectiveness.

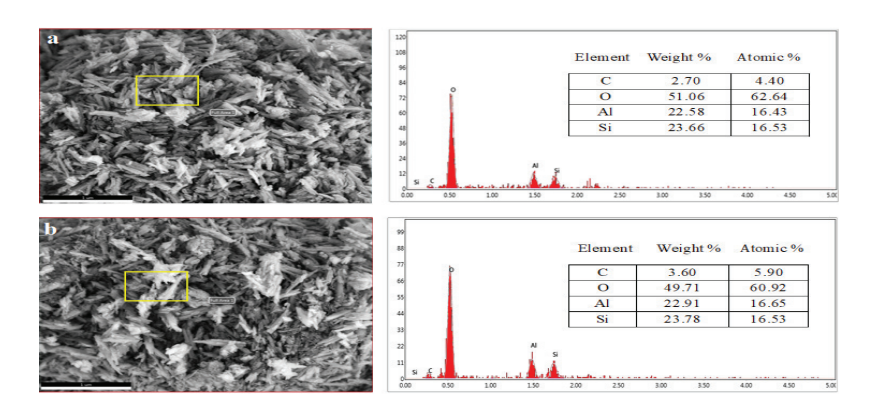


Figure 1: Confirmation of silane treatment by FESEM and EDX of HNTs powder particles; (a) before silane treatment and (b) after silane treatment.

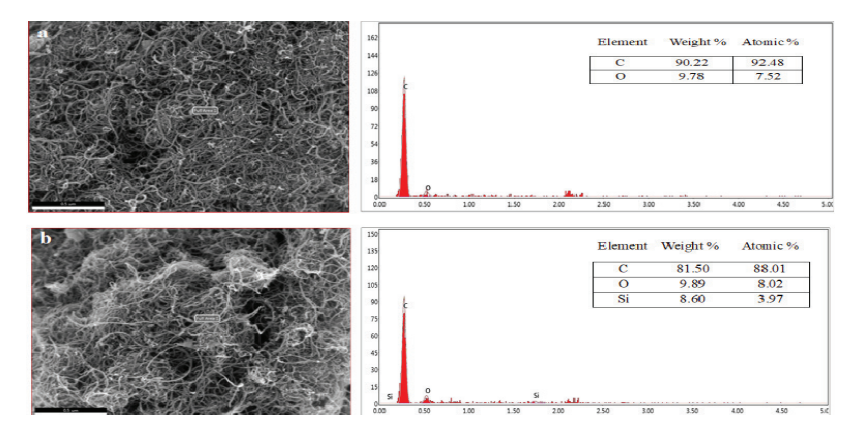


Figure 2: Confirmation of silane treatment by FESEM and EDX of MWCNTs powder particles; (a) before silane treatment and (b) after silane treatment.

4.2 Impact Strength

Figure 3 illustrates the IS results of PMMA composite reinforced with hybrid nanofillers (HNTs/MWCNTs) at varying concentrations, compared to IS of pure PMMA. The results show that PMMA composite with hybrid nanofillers exhibits significantly higher IS compared to pure PMMA (p < 0.05). The highest IS value was achieved with composite in G4 (4.25 wt.% HNTs and 0.75 wt.% MWCNTs), showing a substantial increase to 89.18% (9.97 kJm⁻²) compared to unfilled PMMA (5.27 kJm⁻²). Factors contributing to the increased IS include the formation of crosslinks, enhanced interfacial shear strength and elevated viscosity.^{25,26} Nanda et al. reported a substantial enhancement in IS due to improved impact modifiers, plastic deformation and increased ductile properties of the PMMA matrix.²⁷ Also, the study by Alhotan et al. investigated the impact of E-glass fibres, zirconium dioxide (ZrO₂) and titanium dioxide (TiO₂) nanoparticles on the IS of PMMA bases.² Their findings demonstrated that incorporating E-glass fibres at concentrations of 3 wt.%, 5 wt.% and 7 wt.% in PMMA composites significantly improved IS compared to the control group. The increase in IS is attributed to factors such as uniformity of compound, effective filler infiltration into monomer, strong filler-resin interaction, an optimal filler-to-resin ratio or a combination of organic resin and inorganic filler.²

However, the introduction of high filler loading of MWCNTs, ranging from 1 wt.%–2.5 wt.%, into PMMA composites led to a decrease in IS compared to composites with lower MWCNT levels (less than 1 wt.%), (see Figure 3). Specifically, in G6 and G7, IS values were 7.88 kJm⁻² and 6.79 kJm⁻², respectively, indicating a decline compared to other PMMA reinforced groups. This reduction is attributed to limited compatibility between increasing nanofiller particles and the PMMA matrix, leading to decreased adhesion at the interface. A strong interfacial bond between fillers and matrix is crucial for enhancing IS, as it creates micro-cracks that act as barriers to crack propagation.²⁸ Additionally, the larger surface area of the filler concentrates stress at the aggregation zone, promoting crack propagation.²⁹ These findings align with previous research indicating a decrease in dissipation energy per unit volume at the interface region with increased filler loading and a slight decrease in IS with higher levels of fillers.^{30,31}

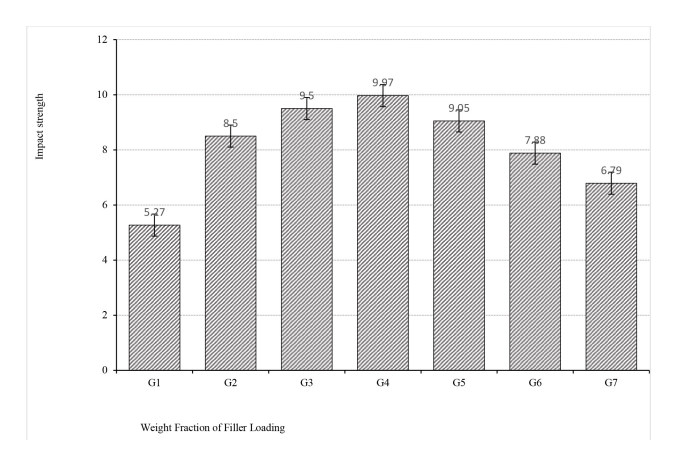


Figure 3: Effects of hybrid nanofillers on IS of PMMA denture base.

4.3 Fracture Toughness

Figure 4 presents data regarding $K_{\rm IC}$ values and variations in both unfilled and filled PMMA, with a 5 wt.% addition of various nanofiller ratios (HNTs/MWCNTs). The results indicated a significant difference (p < 0.05) in $K_{\rm IC}$ between the groups incorporating hybrid nanofillers and the unfilled PMMA, which had 1.60 MPa.m^{1/2}. The PMMA matrix displayed the lowest $K_{\rm IC}$ due to PMMA's inherent brittleness, which reduces strength resistance.^{4,32} The addition of nanoparticles, particularly 4.25% HNTs and 0.75% MWCNTs (G4), to PMMA composites resulted in a substantial increase in the $K_{\rm IC}$ reached 2.65 MPa.m^{1/2}, marking a notable 65.63% improvement with the highest average $K_{\rm IC}$ over unfilled PMMA. Moreover, PMMA composites in G3 and G5 exhibited statistically higher mean $K_{\rm IC}$ values compared to the unfilled PMMA (see Figure 4).

Several factors contributed to enhanced K_{IC} of PMMA composites, including the effective dispersion of nanoparticles within the matrix, strong adhesion between fillers and PMMA matrix, interactions between matrix and fillers, and utilisation of high-strength fillers.³³ These findings are consistent with previous research by Alhotan et al. who observed similar enhancements in K_{IC} within PMMA composites.² Alhotan et al., attributed the rise in K_{IC} to factors such as uniform distribution of compound, successful filler infiltration into monomer, robust connection between filler and resin, optimal filler quantity and synergistic effects between organic resin and inorganic filler. Also, the study demonstrated that lower filler loading of ZrO_2 or TiO_2 at concentrations of 3 wt.% and 5 wt.% into PMMA composites resulted in significantly elevated K_{IC} values, which increased by 23.24% with 5 wt.% ZrO_2 and by 19.72% with 3 wt.% TiO_2 compared to the control group. This increase was

attributed to the uniform distribution of fillers within composite material.² Similar findings were reported by Wang et al., emphasising the importance of a strong bond between filler particles and PMMA matrix for superior mechanical properties in composites.³⁴

Nevertheless, filled PMMA with 2.5:2.5 HNTs/MWCNTs as in G7 showed improvement in K_{IC}, although this enhancement wasn't statistically significant. However, there was a gradual decrease in K_{IC} with an increase in MWCNTs concentration from 1% to 2.5% in the PMMA composites, reaching 1.74 MPa. m^{1/2} when 2.5% MWCNTs were added. Several factors contribute to this decline in PMMA K_{IC}. At higher concentrations, multi-walled carbon nanotubes (MWCNTs) tend to agglomerate due to van der Waals forces acting between the nanotubes. This aggregation reduces the dispersion efficiency within the PMMA matrix. The resulting agglomerates act as defects or stress concentrators, weakening the composite and diminishing its resistance to crack propagation, thereby lowering K_{IC}. When MWCNT content exceeds 1% to 2.5%, the filler-to-matrix interface deteriorates because the available surface area for bonding becomes insufficient. This agglomeration of the matrix prevents additional nanotubes from effectively bonding with PMMA, leading to weak interfaces. These weak interfaces hinder efficient stress transfer, which further reduces K_{IC}. As MWCNT concentrations surpass the optimal threshold, the composite becomes more brittle. A high concentration of fillers restricts the mobility of the polymer chains, limiting the material's capacity to absorb and dissipate energy during fracture, which in turn reduces ductility and makes the material more brittle. Additionally, poorly dispersed MWCNTs in localised regions can cause stress concentrations, which facilitate crack initiation and growth under mechanical stress, further decreasing the K_{IC} of the composite.^{35–38}

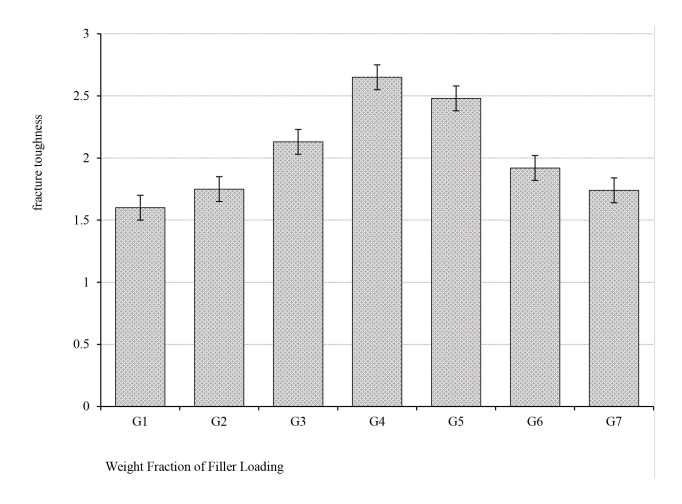


Figure 4: Effects of hybrid nanofillers on K_{IC} of PMMA denture base.

4.4 Artificial Saliva Absorption

Figure 5 and Table 2 illustrate the impact of hybrid nanofiller loading (HNTs/MWCNTs) on the absorption of AS by the PMMA matrix in comparison to pure PMMA (G1). The table compares ASA in percentages and the corresponding ASA values in micrograms per cubic millimetre. These measurements are taken for varying hybrid nanofiller loadings, denoted as G2 through G7 in Table 1. The data pertains to the reinforcement of the PMMA matrix following 28 days of immersion in AS at 37°C. The findings presented in Figure 5 suggest that the reinforced PMMA composite exhibited a slightly higher level of ASA than the pure PMMA matrix and commercial PMMA. The increase in ASA was modest, rising from 1.36% to 1.49%. However, as the hybrid nanofiller loading was added, the ASA diminished. The results also indicate a statistically significant relationship between hybrid nanofiller and ASA, with the reinforced PMMA composite's ASA increasing as more MWCNTs nanofiller was added (*p* < 0.05).

The study results reveal an initial rise in ASA across all formulations during the first phase of the experiment (0–7 days), followed by stability up to 14 days. Beyond the 14 day mark, there was no substantial change in weight until the 28-day mark. The rapid ASA during the first stage (0–7 days) was followed by a final stage (7–21 days) in which the samples reached saturation with the AS solution, resulting in a slight weight reduction. These findings align with those of Raszewski et al. who also observed a similar temporal pattern in AS absorption.³⁹ Furthermore, as indicated in Figure 5, the findings indicate that the PMMA matrix exhibits lower absorption of AS compared to the strengthened PMMA composite after a 28-day immersion at 37°C. Additionally, ASA values for all formulations of the reinforced PMMA composite fall within the acceptable range defined by the ISO 20795-1:2013 guidelines for denture base materials. According to ISO 20795-1:2013, the acceptable water absorption value for denture base polymers should not exceed 32 μgmm⁻³.

Nonetheless, the ASA level in the reinforced PMMA hybrid nanocomposite was slightly higher in comparison to the PMMA matrix. This variation is attributed to increased hydrolytic degradation of the silane interlinking coupling agent, leading to the detachment of filler particles from the matrix.²² The rise in ASA can be traced back to the predominant component in saliva, which plays a significant role in the hydrolytic degradation of the silane coupling agent.²² Furthermore, the introduction of filler loading into the PMMA composite may exacerbate the discrepancy in diffusion coefficients, potentially resulting in the accumulation of AS clusters not only within the matrix but also at the interface between the filler and the matrix, thereby leading to detachment, as discussed by Patti et al.⁴⁰ The hydrolytic degradation observed in the reinforced PMMA composite is attributed to a reduction in the interfacial siloxane bridge bonds connecting the filler and the matrix. This reduction is a consequence of

the hydroxyl ions generated by the hydrolytic degradation of the silanol groups at the interface, as outlined in the work by Shuai et al.⁴¹ The heightened presence of hydroxyl ions exacerbates the breakdown of the silane interface reaction, thereby facilitating the hydrolytic degradation of the reinforced PMMA composite, as discussed in the study conducted by Hemmati et al.⁴²

These findings align with the research conducted by Elshereksi et al. who noted that the deterioration of the silane interface is a catalyst for particle debonding, thereby influencing the characteristics and long-term performance of reinforced PMMA composite materials.²² The increase in AS absorption may also be attributed to the presence of nanofillers within the PMMA matrix, potentially leading to inadequate dispersion of filler particles within the matrix. This, in turn, can result in heightened material porosity and hydrophobicity, rendering it more susceptible to water absorption and solubility when exposed to aqueous environments, such as saliva. These observations are in line with the findings of Rizk et al. and the subsequent research by Elshereksi et al. emphasising the correlation between water absorption properties and the level of porosity and hydrophobicity in materials, with significant implications for material performance in aqueous environments like saliva.^{22,43} Moreover, the hydrophobic characteristics of treated ceramic fillers have been identified as a factor that can mitigate water absorption in composites, as highlighted by Olonisakin et al.44 This conclusion is further substantiated by the research of Zhang and Rong, and Wikant, revealed that when a polymer resin composite is immersed in an aqueous setting, two distinct phases occur. 45,46 Initially, there is a rapid release of uncured monomers, typically completed within a few days. Simultaneously, AS is absorbed by the composite, primarily through diffusion into the polymer matrix. These outcomes strongly imply that the hydrophobic nature of the treated ceramic filler plays a significant role in determining the water absorption properties of the composite and its ability to resist ASA.

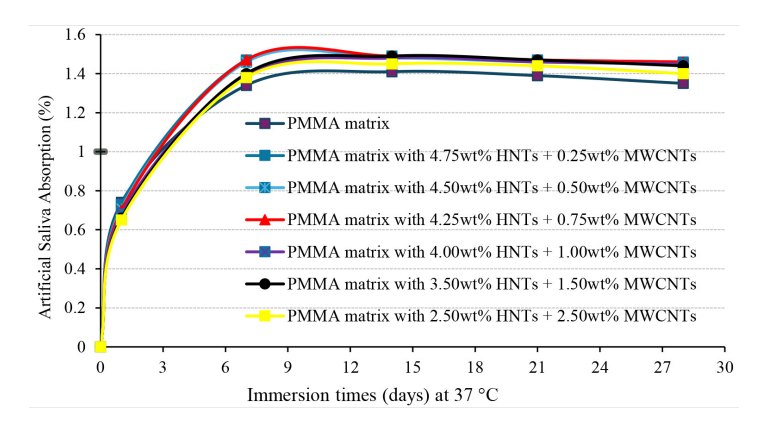


Figure 5: AS curves of PMMA composites filled with nanohybrid filler during 28 days of immersion.

Table 2: AS values of reinforced PMMA with nanohybrid filler compared to PMMA matrix for 28 days of immersion.

Group/Subgroup Code	Amount of ASA (%)	Amount of ASA (µgmm ⁻³)
G1	1.36	21.61
G2	1.49	25.45
G3	1.47	24.65
G4	1.45	23.86
G5	1.43	23.24
G6	1.42	22.74
G7	1.40	22.31

Note: ISO 20795-1:2013 value: max weight increase percentage:1.99%, max weight increases 32 μgmm⁻³.

4.5 Morphology of PMMA Specimen Fracture

The microstructural characteristics of both unfilled and filled PMMA, which included hybrid nanofillers (HNTs/MWCNTs) held at a constant weight percentage of 5%, with varying proportions of each filler, were investigated using FESEM, (see Figures 6-9). The FESEM image of the unfilled PMMA sample displayed a notably smooth surface with small pores, suggesting a brittle fracture (see Figure 6a). This observation aligns with the findings of Sadati et al., who noted that fracture morphology of unaltered PMMA exhibits smooth surface, indicating uncontrolled crack propagation within PMMA matrix.⁴⁷ The fracture surface morphology of PMMA composites in G2 and G3, which incorporated nanofillers, exhibited an uneven texture and displayed small fissures. These characteristics arose from the resistance offered by nanofiller particles to fracture energy (see Figure 6b and Figure 7a). The dispersion of filler particles within the PMMA composite was nearly even, and interaction between these fillers and the PMMA matrix was relatively strong. A rugged fracture surface typically indicates an extended path for crack propagation. This phenomenon can be attributed to various factors, including the material properties of the object being fractured, the applied load or stress conditions, and specific circumstances surrounding the fracture occurrence. 48 Furthermore, variations in the properties of the filler and matrix materials also contribute to the initiation of these microcracks.⁴⁹

The study investigated that PMMA composites in G4 and G5 showed noticeable improvement in the connection between nanofiller and PMMA matrix, evidenced by strong adherence and absence of visible gaps on fractured surfaces (see Figure 7b and Figure 8a). This integration led to increased roughness and ridges on the fracture surface, indicating enhanced resistance to fractures. The addition of γ -MPS further strengthened the bond and improved the uniform distribution of filler particles within the matrix. ⁵⁰ However, in composites with higher concentrations of nanofillers as in G6 and G7, (see Figure 8b and Figure 9), minor gaps and clumping were observed

on the fracture surface, suggesting suboptimal interaction between nanoparticles and PMMA matrix. These imperfections lead to the early formation and expansion of cracks, reducing the material's fracture resistance. This finding corroborates previous research indicating that excessive filler incorporation can lead to large clusters, negatively impacting composite flexibility and strength.⁵¹

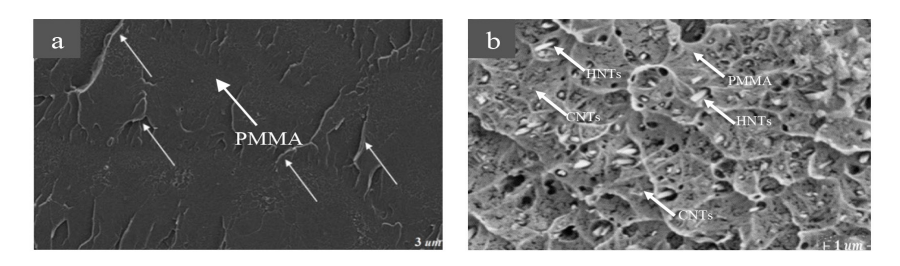


Figure 6: FESEM of the fracture surface of, (a) unreinforced PMMA and (b) PMMA/4.75% HNTs/0.25% CNTs.

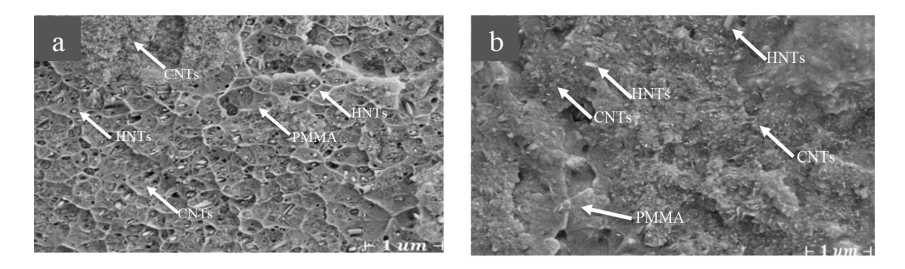


Figure 7: FESEM of the fracture surface of, (a) PMMA/4.5% HNTs/0.5% CNTs and (b) PMMA/4.25% HNTs/0.75% CNTs.

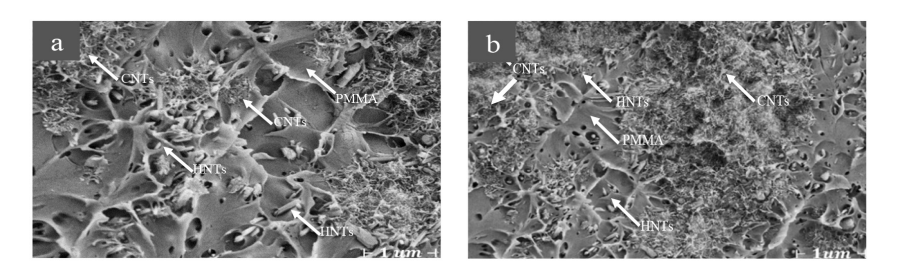


Figure 8: FESEM of the fracture surface of, (a) PMMA/4% HNTs/1% CNTs and (b) PMMA/1.5% HNTs/3.5% CNTs.

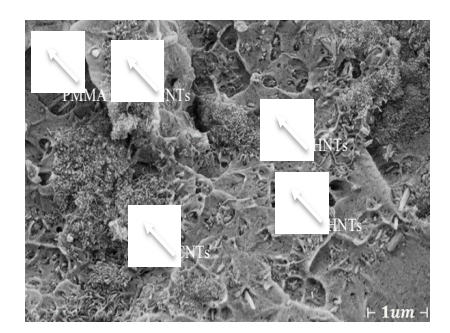


Figure 9: FESEM of the fracture surface of PMMA/2.5% HNTs/2.5% MWCNTs

5. CONCLUSION

The addition of hybrid nanofillers into PMMA composite has demonstrated its effectiveness in enhancing mechanical characteristics such as IS and $K_{\rm IC}$. The ratio of 4.25 wt.% HNTs and 0.75 wt.% MWCNTs exhibited a significant improvement in the PMMA IS and $K_{\rm IC}$ values of 10.26 KJm $^{-2}$ and 2.59 MPa·m $^{1/2}$, respectively, compared to unfiled PMMA. The synergy between these two types of nanotubes, their well-dispersed particles, and their improved adhesion to the PMMA matrix are key factors that play a crucial role in the improved properties of the composite. Consequently, the combination of salinised HNTs/MWCNTs nanotubes as reinforcement agents holds significant potential for augmenting the qualities of PMMA composites.

6. ACKNOWLEDGEMENTS

We would like to sincerely thank Professor Hazizan Md Akil for his invaluable support and guidance while preparing this research. Furthermore, our heartfelt thanks to Ministry of Higher Education in Malaysia and the Polymer Composite Research Centre at Universiti Sains Malaysia for their generous financial assistance in funding this study through the Fundamental Research Grant Number (1001/PBAHAN/8014047).

7. REFERENCES

1. Aati, S. et al. (2022). Silver-loaded mesoporous silica nanoparticles enhanced the mechanical and antimicrobial properties of 3D printed denture base resin. *J. Mech. Behav. Biomed. Mater.*, 134, 105421. https://doi.org/10.1016/j.jmbbm.2022.105421

- 2. Alhotan, A. et al. (2021). Assessing fracture toughness and impact strength of PMMA reinforced with nano-particles and fibre as advanced denture base materials. *Mater.*, 14(15), 4127. https://doi.org/10.3390/ma14154127
- 3. Alageel, O. (2022). Three-dimensional printing technologies for dental prosthesis: A review. *Rapid Prototyp. J.*, 28(9), 1764–1778. https://doi.org/10.1108/RPJ-07-2021-0164
- Ali Sabri, B. et al. (2021). A review on enhancements of PMMA denture base material with different nano-fillers. *Cogent Eng.*, 8(1), 1875968. https://doi.org/10.1080/2331 1916.2021.1875968
- Wang, Z. & Zhitomirsky, I. (2022). Deposition of organic-inorganic nanocomposite coatings for biomedical applications. *Solids*, 3(2), 271–281. https://doi.org/10.3390/ solids3020019
- 6. Gautam, S. et al. (2022). Recent advancements in nanomaterials for biomedical implants. *Biomed. Eng. Adv.*, 3, 100029. https://doi.org/10.1016/j.bea.2022.100029
- 7. Herráez-Galindo, C. et al. (2022). A review on CAD/CAM yttria-stabilized tetragonal zirconia and polymethyl methacrylate and their biological behavior. *Polym.*, 14(5), 906. https://doi.org/10.3390/polym14050906
- 8. Raszewski, Z. et al. (2021). The effect of chlorhexidine disinfectant gels with antidiscoloration systems on color and mechanical properties of PMMA resin for dental applications. *Polym.*, 13(11), 1800. https://doi.org/10.3390/polym13111800
- 9. Bacali, C. et al. (2020). Flexural strength, biocompatibility, and antimicrobial activity of a polymethyl methacrylate denture resin enhanced with graphene and silver nanoparticles. *Clin. Oral Investig.*, 24, 2713–2725. https://doi.org/10.1007/s00784-019-03133-2
- Baba, Z. et al. (2021). CAD/CAM complete denture systems and physical properties: A review of literature. J. Prosthodontics, 30(S2), 113–124. https://doi.org/10.1111/jopr.13243
- 11. Jacob, A. & Prathap, A. (2021). Maxillary Fractures. In K. Bonanthaya, et al. (Ed.). *Oral and Maxillofacial Surgery for the Clinician*. Springer: Singapore, 1125–1149. https://doi.org/10.1007/978-981-15-1346-6_55
- 12. Berlin-Broner, Y. et al. (2023). Implications of post-traumatic treatment of immature maxillary incisors. *Int. Dent. J.*, 73(3), 337–345. https://doi.org/10.1016/j.identj.2023.01.005
- 13. Zidan, H. (2020). Effects of zirconia nanoparticles on the physico-mechanical properties of high-impact heat-cured acrylic resin denture base. PhD diss., The University of Manchester (United Kingdom).
- 14. Chander, G., & Venkatraman, J. (2022). Mechanical properties and surface roughness of chitosan reinforced heat polymerized denture base resin. *J. Prosthodon. Res.*, 66(1), 101–108. https://doi.org/10.2186/jpr.JPR_D_20_00257
- 15. Chladek, G. et al. (2022). Effect of Candida albicans suspension on mechanical properties of denture base acrylic resin. *Mater.*, 15(11), 3841. https://doi.org/10.3390/ma15113841
- 16. Fouly, A. et al. (2021). Effect of low hydroxyapatite loading fraction on mechanical and tribological characteristics of PMMA nanocomposites for dentures. *Polym.*, 13(6), 857. https://doi.org/10.3390/polym13060857

- 17. Zidan, S. et al. (2021). Chemical characterisation of silanised zirconia nanoparticles and their effects on properties of PMMA-zirconia nanocomposites. *Mater.*, 14(12), 3212. https://doi.org/10.3390/ma14123212
- 18. Koo, J. H. (2019). Polymer Nanocomposite Review. In Joseph, H. K. (Ed.). *Polymer Nanocomposites: Processing, Characterization, and Applications*. New York: McGraw Hill.
- 19. Omanović-Mikličanin, E. et al. (2020). Nanocomposites: A brief review. *Health Technol.*, 10, 51–59. https://doi.org/10.1007/s12553-019-00380-x
- Ramburrun, P. et al. (2021). Recent advances in development of antimicrobial and antifouling biocompatible materials for dental applications. *Mater.* 14(12), 3167. https://doi.org/10.3390/ma14123167
- 21. Azmy, E. et al. (2022). Comparative effect of incorporation of ZrO₂, TiO₂, and SiO₂ nanoparticles on strength and surface properties of PMMA denture base material: Vitro study. *Int. J. Biomater.* https://doi.org/10.1155/2022/5856545
- Elshereksi, N. W. et al. (2022). The influence of titanate coupling agent on the performance of barium titanate/PMMA denture base nanocomposites after SBF storage. J. Thermoplas. Compos. Mater., 35(12), 2265–2287. https://doi. org/10.1177/0892705720962160
- 23. Aziz, T. et al. (2021). Recent progress in silane coupling agent with its emerging applications. *J. Polym. Environ.*, 29, 3427–3443. https://doi.org/10.1007/s10924-021-02142-1
- 24. Sabri, M. M. et al. (2023). Scanning electron microscopy as a valuable tool to optimize the properties of the polymer/clay nanocomposites. *Cogent Eng.*, 10(2), 2265231. https://doi.org/10.1080/23311916.2023.2265231
- He, D. et al. (2022). Interfacial coordination interaction enables soft elastomer composites with high thermal conductivity and high toughness. ACS Appl. Mater. Interfaces., 14(29), 33912–33921. https://doi.org/10.1080/23311916.2023.2265231
- 26. Fang, C. et al. (2023). Preparation and characterization of high solid content acrylate latex pressure sensitive adhesives with difunctional cross-linker EGDMA. *Int. J. Adhes. Adhes.*, 125, 103403. https://doi.org/10.1016/j.ijadhadh.2023.103403
- 27. Nanda, T. et al. (2021). Advancements in multi-scale filler reinforced epoxy nanocomposites for improved impact strength: Review. *Critical Reviews in Solid State and Materials Sciences*, 46(4), 281–329. https://doi.org/10.1080/10408436.2020.177 7934
- 28. Al-Saadi, M. et al. (2021). Improving some mechanical properties and thermal conductivity of PMMA polymer by using environmental waste. *Iraqi J. Sci.*, 62(7), 2188–2196. https://doi.org/10.24996/ijs.2021.62.7.8
- 29. Benzait, Z. & Trabzon, L. (2018). A review of recent research on materials used in polymer–matrix composites for body armor application. *J. Compos. Mater.*, 52(23), 3241-3263. https://doi.org/10.1177/0021998318764002
- 30. Hao, S. et al. (2022). Interfacial energy dissipation in bio-inspired graphene nanocomposites. *Compos. Sci. Technol.*, 219, 109216. https://doi.org/10.1016/j.compscitech.2021.109216

- 31. Zhu, X. et al. (2022). The effects of nano-ZrO₂ on the mechanical and electrical properties of silicone rubber and a corresponding mechanism analysis. *IEEE Trans. Dielectr. Electr. Insul.*, 29(6), 2218–2226. https://doi.org/10.1109/TDEI.2022.3203373
- 32. Mousavi, A. et al. (2020). Effects of biocompatible Nanofillers on mixed-mode I and II fracture toughness of PMMA base dentures. *J. Mech. Behav. Biomed. Mater.*, 103, 103566. https://doi.org/10.1016/j.jmbbm.2019.103566
- 33. Nurazzi, M. et al. (2021). Mechanical performance and applications of cnts reinforced polymer composites—A review. *Nanomater.*, 11(9), 2186. https://doi.org/10.3390/nano11092186
- 34. Wang, Y. et al. (2021). Functional fillers for dental resin composites. *Acta Biomater*., 122, 50–65. https://doi.org/10.1016/j.actbio.2020.12.001
- 35. Abushowmi, T. H. et al. (2020). Comparative effect of glass fiber and nano-filler addition on denture repair strength. *J. Prosthodon.*, 29(3), 261–268. https://doi.org/10.1111/jopr.13124
- 36. Mousavi, A. et al. (2020). Effects of biocompatible Nanofillers on mixed-mode I and II fracture toughness of PMMA base dentures. *J. Mech. Behav. Biomed. Mater.*, 103, 103566. https://doi.org/10.1016/j.jmbbm.2019.103566
- Zidan, S. et al. (2019). Investigating the mechanical properties of ZrO₂-impregnated PMMA nanocomposite for denture-based applications. *Mater.*, 12(8), 1344. https://doi.org/10.3390/ma12081344
- 38. Nabhan, A. et al. (2023). Filler loading effect of Al₂O₃/TiO₂ nanoparticles on physical and mechanical characteristics of dental base composite (PMMA). *Polym. Test.*, 117, 107848. https://doi.org/10.1016/j.polymertesting.2022.107848
- 39. Raszewski, Z. et al. (2022). Preparation and characterization of acrylic resins with bioactive glasses. *Scientific Reports*, 12(1), 16624. https://doi.org/10.1038/s41598-022-20840-1
- 40. Patti, A. et al. (2021). The universal usefulness of stearic acid as surface modifier: Applications to the polymer formulations and composite processing. *J. Ind. Eng. Chem.*, 96, 1–33. https://doi.org/10.1016/j.jiec.2021.01.024
- 41. Shuai, C. et al. (2020). Interfacial reinforcement in bioceramic/biopolymer composite bone scaffold: The role of coupling agent. *Colloids Surf. B Biointerfaces*, 193, 111083. https://doi.org/10.1016/j.colsurfb.2020.111083
- 42. Hemmati, F. et al. (2021). Lignocellulosic fiber-reinforced PLA green composites: Effects of chemical fiber treatment. In H. S., Mohamed Thariq, et al. (Eds). *Biocomposite Materials Design and Mechanical Properties Characterization*, 97–204. Springer: Singapore. https://doi.org/10.1007/978-981-33-4091-6_5
- 43. Rizk, S. (2022). Composites structure in dentistry and evolution of filler systems and their effects on properties of composites structure. *Biomater. J.*, 1(6), 22–38.
- 44. Olonisakin, K. et al. (2022). Key improvements in interfacial adhesion and dispersion of fibers/fillers in polymer matrix composites; focus on PLA matrix composites. *Compos. Interfaces*, 29(10), 1071–1120.
- 45. Zhang, M. Q. & Rong, M. Z. (2022). Extrinsic and intrinsic approaches to self-healing polymers and polymer composites. John Wiley & Sons. https://doi.org/10.1002/9781119630005

- 46. Wikant, A. (2023). Dental composites-The effects of matrix composition, suboptimal light curing and water exposure. PhD diss., UiT The Arctic University of Norway.
- 47. Sadati, V. et al. (2022). Experimental investigation and finite element modelling of PMMA/carbon nanotube nanocomposites for bone cement applications. *Soft Matter*, 18(36), 6800–6811. https://doi.org/10.1039/D2SM00637E
- 48. Sharafi, S. et al. (2020). Review of factors that influence fracture toughness of extrusion-based additively manufactured polymer and polymer composites. *Addit. Manuf.*, 38, 101830. https://doi.org/10.1016/j.addma.2020.101830
- 49. Khotbehsara, M. et al. (2020). Effects of ultraviolet solar radiation on the properties of particulate-filled epoxy based polymer coating. *Polym. Degrad. Stab.*, 181, 109352. https://doi.org/10.1016/j.polymdegradstab.2020.109352
- de Menezes, C. et al. (2020). AgVO₃ nanorods silanized with γ-MPS: An alternative for effective dispersion of AgVO₃ in dental acrylic resins improving mechanical properties. Appl. Surf. Sci., 543, 148830. https://doi.org/10.1016/j.apsusc.2020.148830
- 51. Lim, V. et al. (2021). A review on synthesis, properties, and utilities of functionalized carbon nanoparticles for polymer nanocomposites. *Polym.*, 13(20), 3547. https://doi.org/10.3390/polym13203547